

## Real-time, deep-learning aided lensless microscope: supplement

**JIMIN WU,<sup>1</sup>  VIVEK BOOMINATHAN,<sup>2</sup>  ASHOK VEERARAGHAVAN,<sup>2,3</sup>  
AND JACOB T. ROBINSON<sup>1,2,4,\*</sup> **

<sup>1</sup>*Department of Bioengineering, Rice University, Houston, Texas 77005, USA*

<sup>2</sup>*Department of Electrical and Computer Engineering, Rice University, Houston, Texas 77005, USA*

<sup>3</sup>*Department of Computer Science, Rice University, Houston, Texas 77005, USA*

<sup>4</sup>*Department of Neuroscience, Baylor College of Medicine, One Baylor Plaza, Houston, Texas 77030, USA*

\**[jtrobinson@rice.edu](mailto:jtrobinson@rice.edu)*

---

This supplement published with Optica Publishing Group on 10 July 2023 by The Authors under the terms of the [Creative Commons Attribution 4.0 License](#) in the format provided by the authors and unedited. Further distribution of this work must maintain attribution to the author(s) and the published article's title, journal citation, and DOI.

Supplement DOI: <https://doi.org/10.6084/m9.figshare.23607495>

Parent Article DOI: <https://doi.org/10.1364/BOE.490199>

# A real-time, deep-learning aided lensless microscope: supplemental document

This document contains the supplementary material to "A real-time, deep-learning aided lensless microscope".

## 1. PHASE MASK FABRICATION

The phase mask was fabricated using a two-photon photolithography system (Nanoscribe, Photonic Professional GT) with high-resolution dip-in liquid lithography configuration on a 700  $\mu\text{m}$  thick fused silica substrate using a photoresist (Nanoscribe, IP-Dip). The laser power used was 60% of the maximum power, and the laser power and writing speed can be adjusted based on systems. The pattern of the fabricated phase mask can be clearly observed in the monitoring software with proper camera adjustment. After the fabrication, the sample was soaked in SU-8 developer for 20 min, and then soaked in isopropyl alcohol for 2 min then air blow dry. The size of the fabricated phase mask is 3 mm  $\times$  3 mm (Figure S1) to ensure a high light throughput for low-contrast fluorescent samples. The fabricated mask has a pixel size of 1  $\mu\text{m}$  and an overall height of 1.2  $\mu\text{m}$  with a 200 nm height step. Then the fused silica substrate was cut to 5 mm  $\times$  5 mm size to match the designed holder size using a laser cutter.

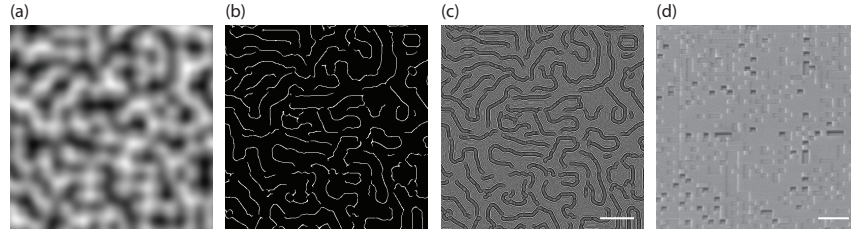


**Fig. S1.** (a) Perlin noise generated for phase mask design. (b) The phase mask pattern was designed by applying Canny edge detection on Perlin noise in panel (a). (c) Height map generated from phase mask pattern by phase retrieving algorithm with designed focal length. Scale bar, 500  $\mu\text{m}$ . (d) Scanned electron micrograph of a fabricated phase mask with 1  $\mu\text{m}$  fabrication pixel size. Scale bar, 5  $\mu\text{m}$ .

## 2. CALIBRATION AND PSFS USED FOR MULTIFLATNET RECONSTRUCTION

The PSFs of the phase mask need to be acquired through the calibration process for the forward model simulation and all the reconstruction methods. For forward model simulation and local convolutional reconstruction, we determined the spacing between each calibration measurement to be 0.5 mm (yellow dots in Figure S2a), which covers a 6 mm  $\times$  6 mm area. Calibration images were captured using a 10  $\mu\text{m}$  pinhole illuminated by a green LED (Thorlabs, M530L4) placed behind an 80-degree holographic diffuser. Five measurements were taken at 100 ms exposure time for each calibration point and averaged to reduce the noise. For MultiFlatNet reconstruction in the main text, we used  $K = 5$  and have five captured PSFs for weights initialization, including the PSF in the center and 4 PSFs at a 3 mm spacing (blue star in Figure S2a). The five PSFs used for MultiFlatNet are shown in Figure S2c, where we could see the shift-variance property of the PSFs.

## 3. THE TRADE-OFF BETWEEN RUN TIME AND RECONSTRUCTION QUALITY

For MultiFlatNet framework, the number of trainable filter weights  $K$  is an important factor determining the reconstruction time cost and quality. A larger number of weights can result in higher reconstruction quality but also increases the run time and memory needs. We tested



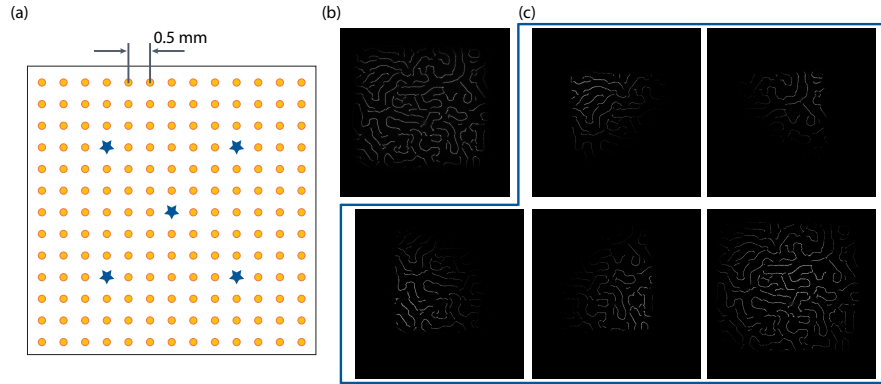


**Fig. S2.** (a) Calibrated positions (yellow dots) and selected positions for weights initialization (blue stars). (b) Aligned and summed up PSF showing the entire pattern generated by the phase mask. (c) Captured PSFs at selected positions (blue stars in panel a). Captured PSFs are brightness enhanced for better visualization.

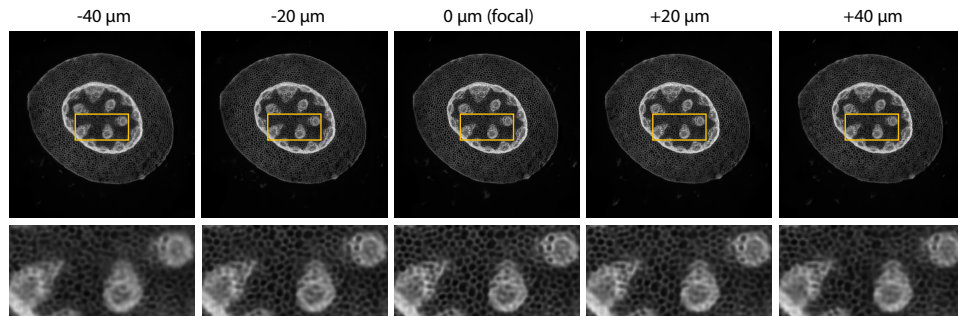


**Fig. S3.** Reconstructions of the same imaging target when capturing at different working distance ( $\pm 20 \mu\text{m}$  and  $\pm 40 \mu\text{m}$  away from the focal depth).

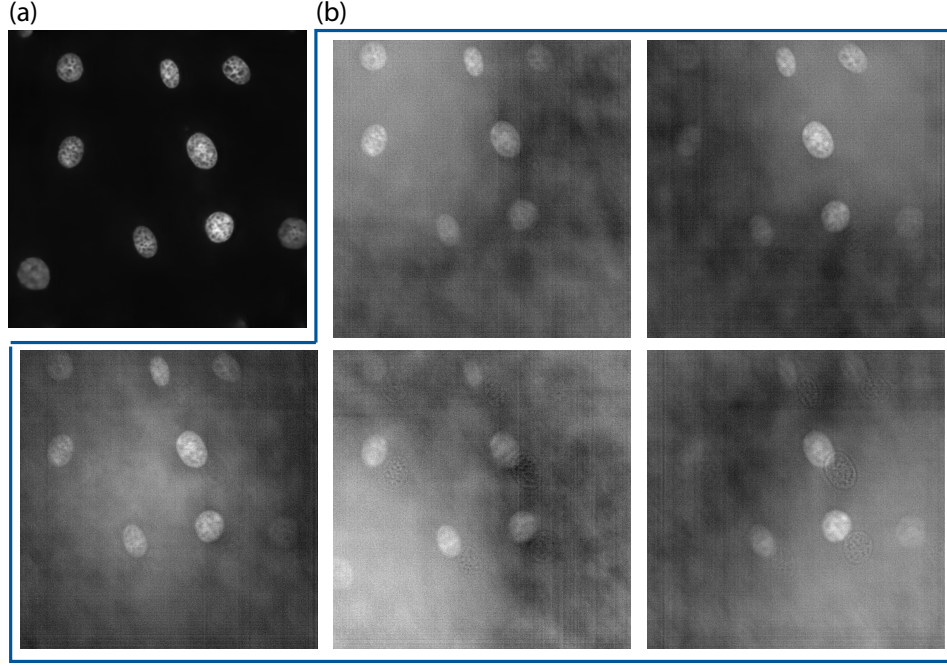


**Fig. S4.** (a) Final reconstructed image using MultiFlatNet. (b) Five output channels from the first stage of MultiFlatNet.

the reconstruction quality and run time using several different  $K$  on simulated captures, and the results are shown in Figure S5 and Table S1. Due to the large memory need, we downsize all the simulated captures and PSFs to  $1024 \times 1024$  pixels. From the results, we could see that increasing the number of weights can improve the image quality, but it leads to significantly increased memory needs.

**Table S1.** Average Metrics on Simulated Testing Dataset

Number of weights	PSNR (in dB)	Runtime (s)
$K = 1$	20.14	0.0162
$K = 5$	26.25	0.0261
$K = 9$	26.34	0.0304
$K = 13$	26.57	0.0374

#### 4. USER INTERFACE DESIGN

We developed a simple and easy-to-use user interface for the usability study. The designed user interface is shown in Figure S6. This user interface is capable of real-time display of the capture and MultiFlatNet reconstruction of the lensless microscope and can save the current capture and reconstruction. Camera settings (e.g. exposure time, gain, gamma) can be changed in the ‘Device’ panel. The current user interface can meet the basic need of microscope users, and more functions can be added in the future. The current display frame rate is around 10 fps on a workstation with an 8-core processor (AMD Ryzen 7 3700X, 3.59GHz), 64 GB RAM, and the reconstruction algorithm was run on Nvidia GeForce RTX 2070 GPU. The limited frame rate is caused by the limited speed of extracting frames of the current CMOS sensor. A higher frame rate can be achieved if using a different sensor or making the model executable.

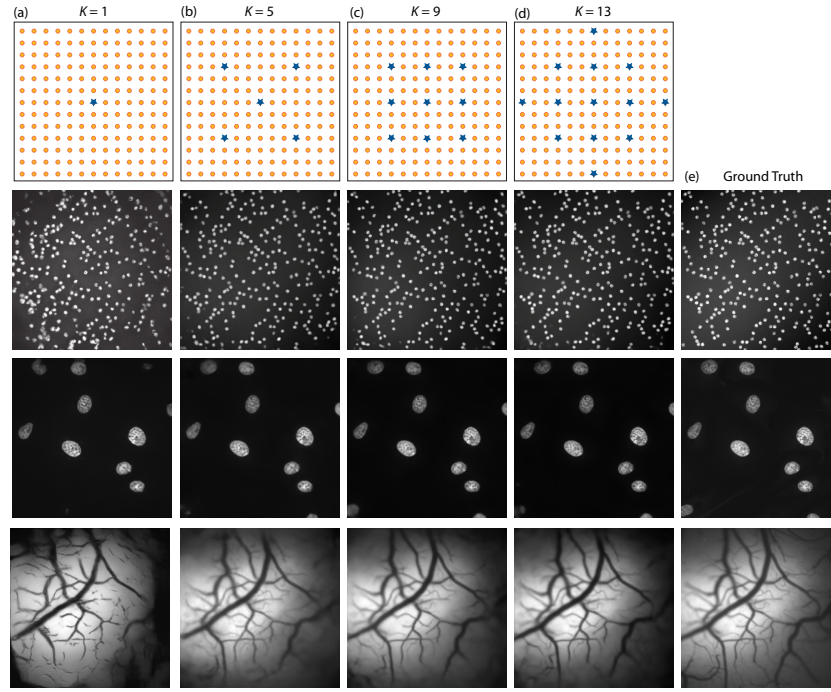


**Fig. S5.** (a) Selected PSF position for weights initialization and sample reconstructions when  $K = 1$ . (b) Selected PSF positions for weights initialization and sample reconstructions when  $K = 5$ . (c) Selected PSF positions for weights initialization and sample reconstructions when  $K = 9$ . (d) Selected PSF positions for weights initialization and sample reconstructions when  $K = 13$ . (e) Ground truth images.

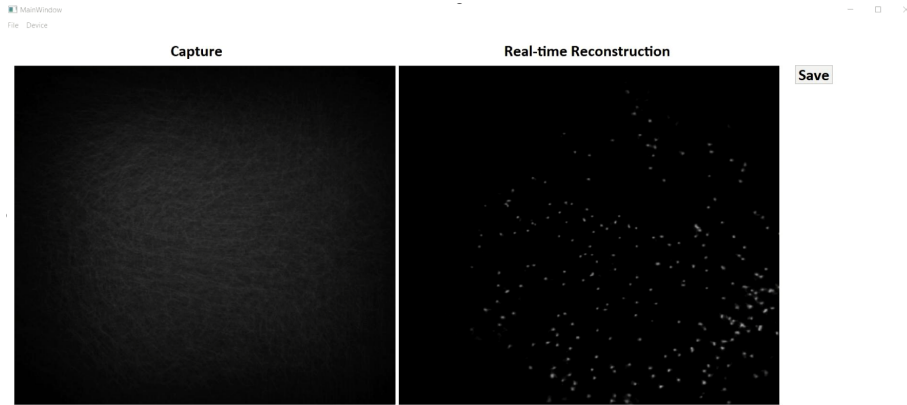


**Fig. S6.** A screenshot of the designed user interface when imaging a sample containing 15  $\mu\text{m}$  fluorescent beads.

## 5. USABILITY STUDY SETUPS

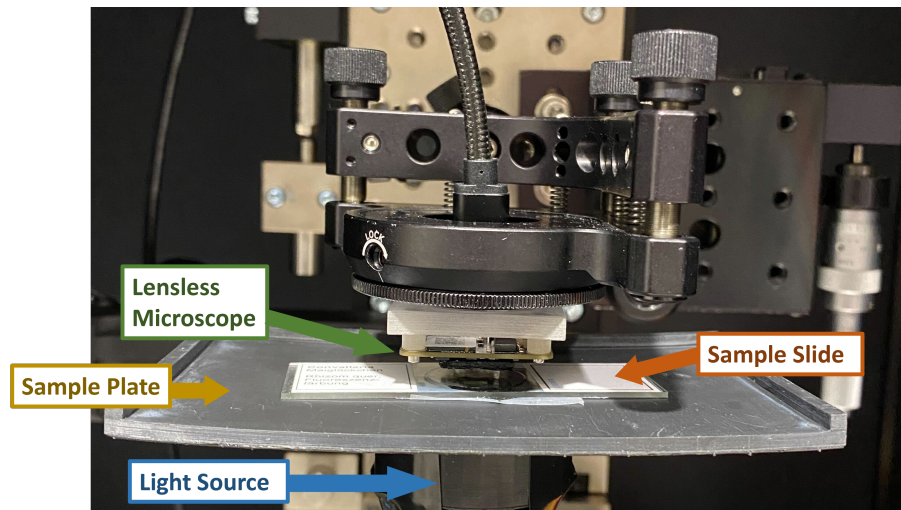


**Fig. S7.** Experimental setup of the usability study.